Electric Field Dependency of Dielectric Behavior of Thermally Sprayed Ceramic Coatings

Minna Niittymäki and Kari Lahti
Department of Electrical Engineering
Tampere University of Technology
Tampere, Finland
minna.niittymaki@tut.fi

Tomi Suhonen and Jarkko Metsäjoki
Advanced Materials
VTT Technical Research Centre of Finland
Espoo, Finland

***Abstract*— High temperature applications e.g. fuel cells require ceramic based insulation solutions instead of polymers. The aim of this paper was to characterize the dielectric properties of thermally sprayed ceramic coatings; especially the electric field dependency of AC and DC behavior of thermally sprayed ceramic coatings. One of the spinel samples and one of the alumina samples have quite similar lamellar microstructure which may partly explain their similar type of behavior in DC resistivity as well as in AC loss indexes at low frequencies. These two samples had smaller lamellar size than the other alumina and spinel samples which also had quite similar behavior of AC losses at low frequencies, respectively. In addition to the lamellar size and structure, also micro cracks in the coating microstructure are proposed to have an effect on the dielectric behavior and its electric field dependency.**

Keywords*— *thermal spraying; HVOF; ceramic; coating; alumina; spinel; dielectric spectroscopy; dc conductivity; loss index; resistivity; breakdown

I. INTRODUCTION

High temperature applications such as fuel cells require ceramic based insulation solutions instead of polymers. Thermal spraying is a fast and relatively inexpensive method for producing electrical insulation for demanding application conditions and geometries. While various materials can be thermally sprayed, in electrical insulation applications the commonly used materials are alumina (Al_2O_3) and magnesium aluminate ($MgAl_2O_4$). Although there are clear needs and applications for electrically insulating coating materials, the previous studies of the dielectric properties of thermally sprayed ceramic coatings are focused on dielectric breakdown properties and only a few studies on dc conductivity, relative permittivity and dielectric losses can be found in the literature [1]–[7]. However, previous studies on the DC conductivity of thermally sprayed coatings typically indicate that the conductivity quite typically increases non-linearly already at quite low electric fields [5]. Thus the aim of this paper is to study the DC resistivity and especially the relative permittivity and dielectric losses of thermally sprayed alumina and magnesium aluminate coatings as a function of electric field. All such studies have to be carried out at controlled conditions because ambient conditions have major influence on the dielectric properties of thermally sprayed ceramic coatings [1], [4], [6]. Because the coatings have special microstructure which most probably has a remarkable effect on the dielectric properties [1], the influence of the microstructure of the studied coatings on the DC and AC behavior is analyzed.

978-1-4799-8903-4/15/$31.00 ©2015 IEEE

II. EXPERIMENTAL

A. Studied Materials

The coatings were manufactured from two commercial alumina (Al_2O_3) powders and two different experimental spinel ($MgAl_2O_4$) powders which were sprayed by high-velocity-oxygen-fuel (HVOF) technique on stainless steel substrates. The difference in Al_2O_3 powders was different particle size, HVOF2 powder has smaller particle size (2-10 μm) than HVOF3 (5-25 μm). $MgAl_2O_4$ coating HVOF1 was sprayed from Al_2O_3-MgO composite powder which formed into a spinel coating during the spraying process. However, the other $MgAl_2O_4$ coating (HVOF4) was sprayed from a spinel form $MgAl_2O_4$ powder.

When the powder particles are heated and accelerated towards the substrate in the spraying process, melted particles form droplets which splat on the substrate/coating surface forming a coating consisting of splats with interfaces in between. The surfaces of the splats cool down faster than the internal parts, and due to this the surfaces are normally more amorphous areas while the internal parts are typically more crystalline. These splats form the lamellae of a coating but the coating exhibits also defects e.g. voids as well as some cracks. During the cooling at least some vertical cracks are rather easily formed in the coating, which are typically problematic for electrical insulation materials. However, thermally sprayed coatings exhibit quite typically at least some vertical cracks but the length and amount of the cracks play an important role. It can be noticed from Fig. 1 that the spinel sample HVOF1 and the alumina sample HVOF2 exhibit quite similar lamellar microstructure where clear crystalline (lighter) and amorphous (darker) areas can be seen. However, alumina sample HVOF3 has only small amount of amorphous areas and spinel sample HVOF4 has significantly smaller amount of amorphous areas than the other spinel HVOF1. In addition, HVOF1 and HVOF2 samples have smaller lamellar size than the alumina sample HVOF3 and the spinel sample HVOF 4.

The coating thicknesses of the samples were defined by magnetic measuring device (Elcometer 456B) and from cross-section surface images taken by optical micrographs [7]. In the magnetic measurements the mean values and the experimental standard deviations of the thicknesses were calculated from 10

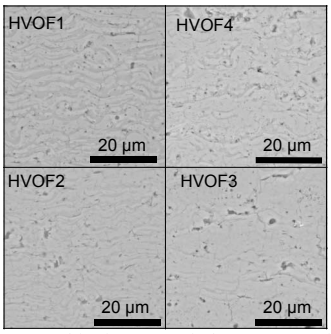

Fig.1.SEM/BSE micrographic images of the cross-sections of the studied coatings.

parallel measurements covering the electrode area used in the DC resistivity and dielectric spectroscopy measurements. The coating thickness values have quite large deviation partly due to the grit blasting made for the steel substrates, which makes the surface of the rather unsmooth.

Porosity values of the coatings were defined by image analysis from optical micrographs (OM) and from scanning electron microscope (SEM) by two detectors secondary electron (SE) and backscattering electron (BSE) [7] which are presented in Table I. In addition, the thickness values and gas (nitrogen) permeability of the coatings are presented in Table I. Typically, higher gas permeability indicates more porous material, but as it can be seen from Table I alumina sample HVOF3 has very high gas permeability in comparison to the other samples although the porosity values are at quite similar level with the others. This difference is most probably due to the vertical cracks seen in the microstructure image of the coating HVOF3 (Fig.1).

B. Sample Preparation and Test Procedures

For the DC resistivity and relative permittivity measurements, a round silver electrode (∅=50 mm) was painted on the middle of a coating sample. In addition, a shield electrode was painted around the measuring electrode to neglect possible surface currents. For breakdown measurements silver electrodes (∅=11 mm) were painted on the sample surface to improve the contact between the voltage electrode and the coating. The used silver paint (SPI Conductive Silver Paint) did not penetrate into the coating [7]. After painting the electrodes the samples were at first dried at 120 °C for two hours followed by conditioning at climate room at 20 °C, RH 20 % for at least 12 h before the measurements. All the measurements for the samples were also performed in the climate room at above the mentioned conditions.

TABLE I. THICKNESS, POROSITY AND GAS PERMEABILITY VALUES FOR THE STUDIED COATINGS USING DIFFERENT MEASUREMENT METHODS.

	Sample	**HVOF 2**	**HVOF 3**	**HVOF 1**	**HVOF 4**
	Composition	Al_2O_3	Al_2O_3	MgO-Al_2O_3	$MgAl_2O_4$
Thickness	From magnetic meas. mean (µm)	208	281	130	196
	From magnetic meas. SD (µm)	3.9	9.1	3.1	3.4
	From cross-section image (µm)	209	288	125	195
Porosity	OM (%)	1.9	1.7	0.9	1.3
	SEM/SE (%)	1.0	1.0	0.6	1.3
	SEM/BSE (%)	1.9	3.0	1.4	2.4
	Gas permeability (nm^2)	5.7	19.2	3.0	3.2

C. DC Resistivity Measurements

Resistivity measurements were made using Keithley 6517B electrometer. The test voltage was maintained until a stabilized current level (i.e. pure resistive current) was reached. In practice, the tests were performed at test voltages ranging from 10 V to 1000 V in order to study the resistivity as a function of electric field. The stabilized DC current was measured 1000 s after the voltage application. All the measuring arrangements were in accordance with the standards IEC 60093/ASTM D257-07.

D. Dielectric Spectroscopy

Relative permittivity and dielectric losses of the materials were studied with an insulation diagnosis analyzer device (IDA 200, U_{max}=200 V_{peak}) and its high voltage unit (IDA HV unit, U_{max}=30 kV_{peak}). During the measurements, a sinusoidal voltage with varying frequency was applied over the sample. The measuring electric field varied from 0.1 V/µm to 5 V/µm. The measuring electric field was limited to quite low levels (corresponding possible service stress levels) to ensure that samples will not break down during the measurements.

The complex impedance of a sample was calculated from the measured test voltage and the current through a sample which was expressed by IDA device as the equivalent parallel RC circuit model. The relative permittivity (ε_r) and dissipation factor (*tan* δ) were calculated from the measured parallel resistance and capacitance using Eq. 1-2, where C_p is measured parallel capacitance and R_p parallel resistance of the equivalent circuit model of a dielectric. C_0 is the so-called geometric capacitance of the test sample (vacuum in place of the insulation) and ω is the angular frequency. The edge field correction (C_e) was not used because the shield electrode was utilized in the measurements. Loss index (ε_r'') includes all the losses of a sample: both conductive and dielectric ones. It can be defined from relative permittivity and dissipation factor, *tan* δ, with Eq.3. All the test arrangements were performed in accordance with the IEC standard 60250.

$$\varepsilon_r \approx \varepsilon_r' = \frac{C_p}{C_0} - \frac{C_e}{C_0}, \quad (1)$$

$$\tan\delta = \frac{1}{R_p C_0 \omega}, \quad (2)$$

$$\varepsilon_r'' = \varepsilon_r \tan\delta \quad (3)$$

E. DC Breakdown Strength Measurements

DC breakdown (bd) voltage measurements were made with a linearly ramped DC voltage. Oil immersion was not used in the measurements because the coatings are porous allowing oil to penetrate into the coating which significantly affects the breakdown strength [7]. During the breakdown tests, the samples were clamped between two stainless steel electrodes: a flat-ended rod (∅= 11 mm) and a flat plate (∅=50 mm). A software controlled linear ramp rate of 100 V/s was used throughout the test until breakdown occurred. Dielectric breakdown field strength of a coating was calculated dividing

the breakdown voltage by the corresponding coating thickness at the painted electrode (∅=11 mm) location.

III. Results and Discussion

A. DC Resistivity

Figure 2 presents the DC resistivity of the studied alumina and spinel coatings as a function of electric field. It can be noticed that all the samples have non-ohmic behavior already at quite low electric field values (approximately ≥ 0.5 V/µm) as it was also reported in [5], [6].

It can be observed that the resistivity of alumina HVOF3 is almost one decade lower than the resistivity of the other studied coatings. This is most probably due to the notable vertical cracks of the sample which probably is also one reason, together with the voids, for the high gas permeability value of this sample. The larger powder particle size of HVOF3 coating may also partly explain the difference in resistivity of the alumina samples, since it may lead to the thicker coating lamellae observable in Fig.1. The DC resistivity of MgO-Al_2O_3 sample (HVOF1) is at very similar level with the Al_2O_3 sample HVOF2, but the spinel HVOF4 sample has lower resistivity above the electric field of 0.5 V/µm. This difference in HVOF4 may be partly due to the larger size of lamellae than in HVOF1 (Fig.1).

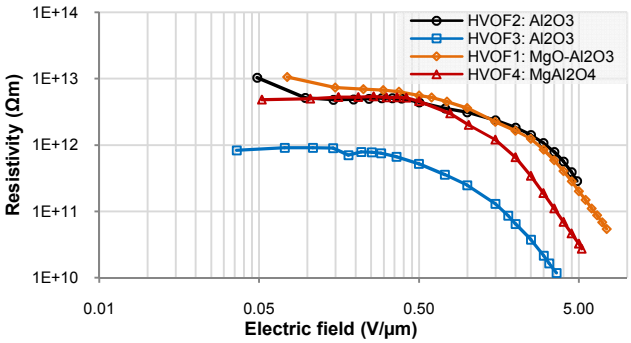

Fig. 2. DC resistivity of the studied materials as a function of electric field.

B. Dielectric Spectroscopy

Figure 3a-b presents the relative permittivity of the studied alumina and spinel coatings. At the frequency of 100 Hz the relative permittivity of all samples are ~10 at all the electric field strengths. At the lower frequency (0.1 Hz), lowest relative permittivity was measured for MgO-Al_2O_3 sample (HVOF1) and the permittivity does not increase with increasing electric field unlike in the case of $MgAl_2O_4$ sample (HVOF4). Alumina sample made from smaller particle size powder (HVOF2) has lower relative permittivity at 0.1 Hz than the other alumina sample (HVOF3) made from larger particle size powder. The permittivity of both alumina samples increase slightly with increasing electric field but the effect is quite small.

The loss indexes of all the coatings at the frequency of 100 Hz are approximately at similar level (Fig. 3c-d). However, at the frequency of 0.1 Hz the loss indexes of alumina and spinel samples differ significantly. Alumina sample HVOF2 and spinel sample HVOF1 are only slightly dependent on the electric field at 0.1 Hz. In addition, the alumina sample (HVOF2) has higher loss index than the spinel sample (HVOF1). The loss index of alumina sample HVOF3 and spinel sample HVOF4 are dependent on the electric field especially above 0.5 V/µm. As it can be noticed from Fig. 1, the spinel sample HVOF1 and the alumina sample HVOF2 exhibit quite similar lamellar microstructure which may explain their similar type of behavior in DC resistivity as well as in AC loss indexes at low frequencies. These two samples

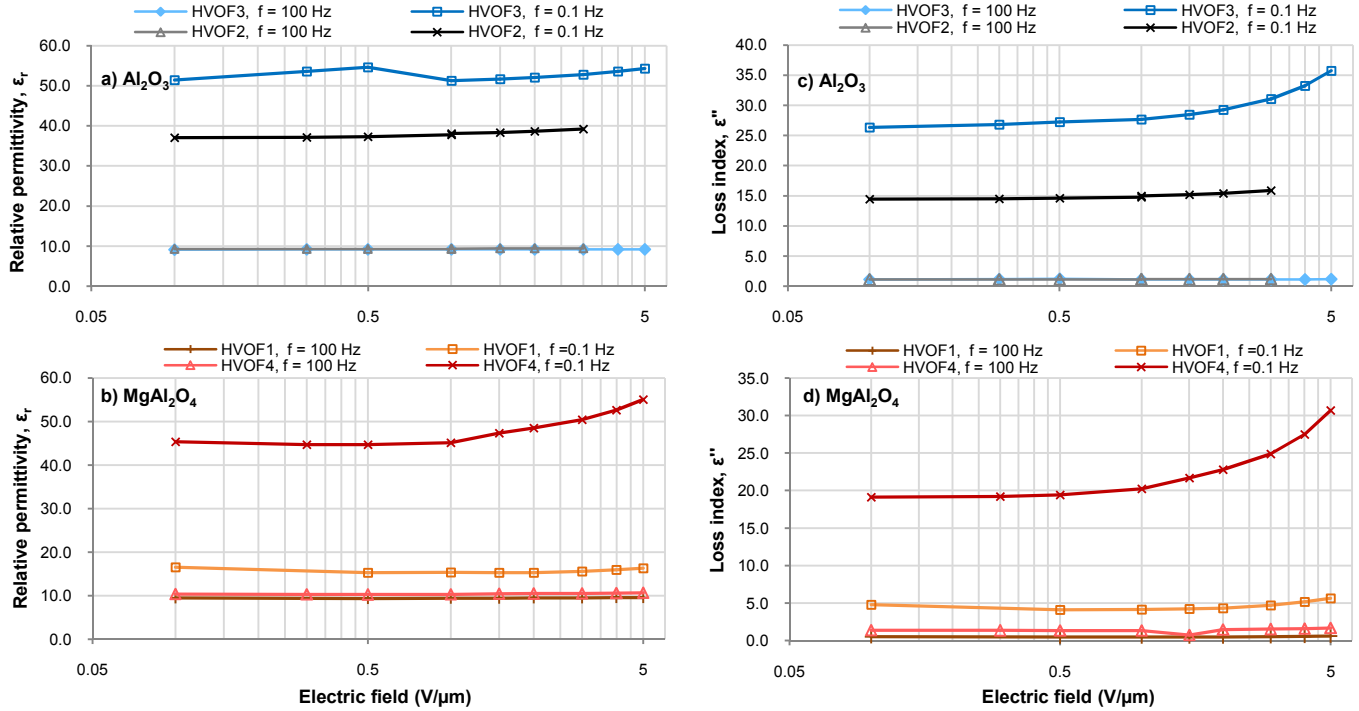

Fig.3. Relative permittivity of a) alumina and b) spinel coatings as a function of electric field. Loss index of c) alumina samples and d) spinel samples with two frequencies as a function of electric field.

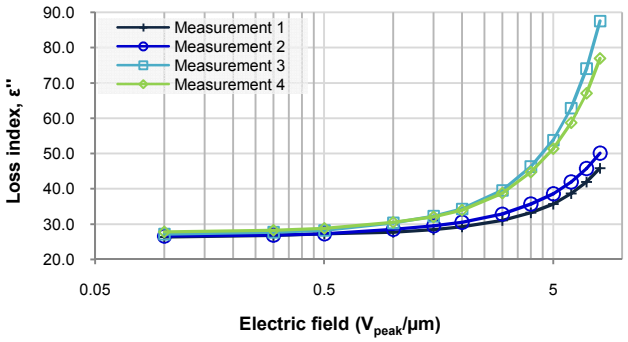

Fig. 4. Loss index of sample HVOF3 at frequency of 0.1 Hz as a function electric field after different measurements.

have smaller lamellar size and the amount of amorphous areas is higher than in the HVOF3 and HVOF 4 which in turn have quite similar behavior in AC losses at low frequencies although the actual values differ.

Because DC resistivity measurements caused some permanent changes to the thermally sprayed ceramics in [6], dielectric spectroscopy measurements were remade for the studied samples in order to verify the possible permanent changes. The samples were placed again in controlled conditions (20°C, RH 20%) and the measurements were remade on the next day. This procedure was repeated for all the studied samples two times and the changes in the AC losses were significant especially in the case of sample HVOF3 which was measured four times due to this. Figure 4 shows the loss index of HVOF3 at a frequency of 0.1 Hz as a function of electric field from the first measurement to the fourth.

It can be observed that at low electric fields (below 1 V/µm), the loss indexes are at similar level in the different measurements, but at higher field strengths the loss indexes increased notably after the second measurement. Thus some permanent changes occurred in the material, probably some of the vertical cracks inside the coating broke into more conducting state short circuiting part of the lamellae, which further changed the capacitance of the coating and increased the conductivity. Since certain field strength is required for the short circuiting, the behavior at lower field strengths is repeatable. The loss index of the other alumina coating (HVOF2) increased in a quite similar way indicating similar permanent material changes. However, the loss index and relative permittivity of the spinel samples (HVOF1 and HVOF4) did not increase like the properties of alumina most probably due to the fewer amount of micro cracks.

C. DC Breakdown Strength

Table II shows the mean dielectric breakdown strength from five parallel measurements for all the studied coatings as well as the corresponding experimental standard deviations. The MgO-Al_2O_3 coating (HVOF1) has the highest breakdown strength but on the other hand the deviation is also the highest. However, the other spinel sample (HVOF4) has notably lower DBS probably because of the different lamellar size (Fig. 1). Despite the highest DC conductivity and measured material degradation during the characterizations, the alumina sample

TABLE II. MEAN BREAKDOWN STRENGTH AND EXPERIMENTAL STANDARD DEVIATIONS FOR THE STUDIED COATINGS.

Sample	Mean DBS (V/µm)	SD (V/µm)
HVOF1: MgO-Al_2O_3	30.2	5.3
HVOF4: $MgAl_2O_4$	19.3	3.7
HVOF2: Al_2O_3	21.6	4.4
HVOF3: Al_2O_3	25.1	2.7

HVOF3 has higher DBS in comparison to the other alumina (HVOF2).

IV. CONCLUSIONS

Microstructural properties of thermally sprayed ceramic coatings have been discussed as well as the role of these properties on their electrical behavior. Particularly, vertical micro cracks are suggested to be one reason for the noticed non-linearity along the applied field strength. In addition, size of lamellae and the amount of amorphous areas may also have significant effect on the dielectric properties, especially in AC loss indexes at low frequencies and in DC resistivity. In general, the spinel samples had lower AC loss indexes than alumina samples. In addition, the DC resistivity was typically higher than that of alumina coating which is in line with the AC behavior.

The studied coatings were tested as-sprayed without any electrical pre-stressing. In the dielectric spectroscopy measurements of alumina coatings certain permanent changes occurred already at rather low field strengths representing realistic service stresses. Thus, in order to reflect better real application behavior, it is recommended to make some electrical pre-stressing prior to the characterizations.

REFERENCES

[1] F. L. Toma, S. Scheitz, L. M. Berger, V. Sauchuk, M. Kusnezoff, and S. Thiele, "Comparative study of the electrical properties and characteristics of thermally sprayed alumina and spinel coatings," *J. Therm. Spray Technol.*, vol. 20, no. 1–2, pp. 195–204, 2011.

[2] F.-L. Toma, L. M. Berger, S. Scheitz, S. Langner, C. Rödel, A. Potthoff, V. Sauchuk, and M. Kusnezoff, "Comparison of the Microstructural Characteristics and Electrical Properties of Thermally Sprayed Al 2O 3 Coatings from Aqueous Suspensions and Feedstock Powders," *J. Therm. Spray Technol.*, vol. 21, no. 3–4, pp. 480–488, 2012.

[3] L. Pawłowski, "The relationship between structure and dielectric properties in plasma-sprayed alumina coatings," *Surf. Coatings Technol.*, vol. 35, no. 3–4, pp. 285–298, 1988.

[4] M. Niittymäki, B. Rotthier, T. Suhonen, J. Metsäjoki, and K. Lahti, "Effects of ambient conditions on the dielectric properties of thermally sprayed ceramic coatings," in *Proceedings of the 23th Nordic Insulation Symposium Nord-IS 2013*, 2013, pp. 131–135.

[5] M. Niittymäki, K. Lahti, T. Suhonen, U. Kanerva, and J. Metsäjoki, "Dielectric properties of HVOF sprayed ceramic coatings," in *Proceedings of the IEEE International Conference on Solid Dielectrics*, 2013, pp. 389–392.

[6] M. Niittymäki, T. Suhonen, J. Metsäjoki, and K. Lahti, "Influence of Humidity and Temperature on the Dielectric Properties of Thermally Sprayed Ceramic MgAl2O4 Coatings," in *2014 Annual Report Conference on Electrical Insulation and Dielectric Phenomena*, 2014, pp. 94–97.

[7] M. Niittymäki, K. Lahti, T. Suhonen, and J. Metsäjoki, "Dielectric Breakdown Strength of Thermally Sprayed Ceramic Coatings: Effects of Different Test Arrangements," *J. Therm. Spray Technol.*, vol. 24, no. 3, pp. 542–551, Jan. 2015.